Electron correlation, d-band formation, and magnetism in V_5S_8: Photoemission-spectroscopy study

A. Fujimori

Department of Physics, University of Tokyo, Bunkyo-ku, Tokyo 113, Japan

M. Saeki and H. Nozaki

National Institute for Research in Inorganic Materials, Tsukuba, Ibaraki 305, Japan

We have studied the electronic structure of a metallic antiferromagnet V_5S_8 above the Néel temperature by photoemission spectroscopy. The V $3s$ core-level peak shows a splitting dominated by the exchange splitting resulting from the high-spin $d^2(V^{3+})$ configuration in the ground state. On the contrary, the valence-band photoemission spectra are in good agreement with band-structure calculations that show a high density of states at the Fermi level. In order to reconcile these apparently contradictory results, we propose that the on-site d-d Coulomb energy is effectively reduced from the average Coulomb energy through Hund's-rule coupling and that this leads to the metallic state even though the average Coulomb energy may be comparable to or exceed the one-electron V $3d$-t_{2g} band width. While the local-moment picture is sufficient to explain the paramagnetic state, itinerant character also has to be taken into account to consider the antiferromagnetic state.

I. INTRODUCTION

Electron correlation in narrow-band metals has been the subject of extensive research in solid-state physics. In the metallic V-S system, the degree of d-electron localization can be varied through changing the composition between VS and V_5S_8: VS and V_3S_4 show weak temperature-independent paramagnetism,[1] whereas V_5S_8 shows Curie-Weiss behavior above the Néel temperature.[1-3] V_3S_4 and V_5S_8 order antiferromagnetically below $T_N = 8$ (Ref. 4) and 32 K,[1-3] respectively. Since the V $3d$ electrons are thought to be responsible for both metallic conductivity[5] and magnetism, it has been controversial whether the magnetism is of the itinerant-electron type or local-moment type.[1-4,6,7]

In the present work, we have investigated the electronic structure of V_5S_8 by photoemission spectroscopy in order to get insight into the nature of electron correlation and magnetism. V_5S_8 has a monoclinic structure derived from the metal-deficient NiAs-type structure[8] as shown in Fig. 1: V vacancies occur in every second metal layer; the V atoms in the vacancy layers are ordered, resulting in three types of V sites (V^I, V^{II}, and V^{III}). This structure can also be viewed as a layered compound VS_2 intercalated with V^I atoms, i.e., $V_{0.25}VS_2$. Nuclear-magnetic-resonance (NMR) studies have shown that only V atoms in the vacancy layers V^I have magnetic moments.[7] From their NMR experiments, Kitaoka and Yasuoka[1] have deduced an ordered moment of $0.22\mu_B$ at the V^I site. As this value is much smaller than the effective moment of the paramagnetic state, $\sim 2.3\mu_B$, these authors have proposed that the antiferromagnetism is of itinerant-electron type. A neutron-diffraction study by Funahashi *et al.*,[6] on the other hand, has yielded a larger ordered moment

$[(0.7-1.5)\mu_B]$ at the V^I site, favoring a local-moment picture.

Our spectra have shown both local-moment-like and bandlike features for V $3d$ electrons depending on the energy level studied. In order to reconcile these apparently contradictory results, we propose that the effective reduction of the on-site d-d Coulomb energy through the intra-atomic exchange interaction (Hund's-rule coupling) serves to stabilize the metallic d-band formation. We have discussed the implications of the previous and present results for the anomalous magnetic properties of
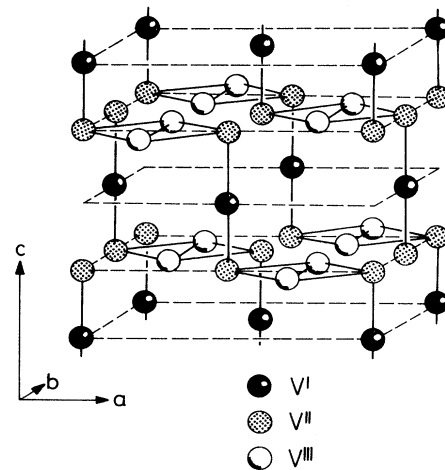
FIG. 1. Arrangement of V atoms in V_5S_8. The structure is distorted from the ideal metal-deficient NiAs structure. V-V bonds shorter than 3.1 Å are indicated by solid lines (Ref. 8).

V_5S_8, and concluded that itinerant character of d electrons becomes important for the V^I site in going from the paramagnetic to the antiferromagnetic states.

II. EXPERIMENTAL

A single crystal of V_5S_8 was grown by the chemical transport method.[9] The composition was determined to be $VS_{1.64}$, which is in the homogeneity range of the V_5S_8 phase, namely, between $VS_{1.57}$ and $VS_{1.64}$.

Photoemission experiments were carried out using a spectrometer equipped with a Mg x-ray source (Mg $K\alpha$: $h\nu = 1253.6$ eV) for x-ray photoemission spectroscopy (XPS) and a He discharge lamp (He I: $h\nu = 21.2$ eV and He II: 40.8 eV) for ultraviolet photoemission spectroscopy (UPS). In order to obtain clean surfaces, the sample was scraped in situ with a diamond file. No oxygen $1s$ core-level peak (at binding energy $E_B \sim 530$ eV) and carbon $1s$ core-level peak was detected by XPS, and no oxygen $2p$ emission in the valence band UPS. Measurements were performed at room temperature, well above T_N. Auger-electron spectra were recorded using the Mg $K\alpha$ line as an excitation source.

The energy resolution was ~ 1 and ~ 0.2 eV for XPS and UPS, respectively. For XPS, the natural width of the Mg $K\alpha$ line is $2\gamma = 0.36$ eV at full width at half maximum (FWHM).[10] The resolution of the analyzer (operated with a pass energy of 25 eV) plus unresolved Mg $K\alpha_1$ and $K\alpha_2$ lines can be represented by a Gaussian FWHM of $2G = 0.8$ eV, which will be taken into account in the following line-shape analyses.

III. RESULTS

A. Core levels

Sulfur core-level photoemission spectra of V_5S_8 are found to have simple line shapes. Figure 2 shows that the

S $2p$ core-level spectrum can be fitted using a single spin-orbit doublet accompanied by a plasmon satellite.

Vanadium core-level spectra, on the other hand, exhibit complex line shapes. The V $3s$ core-level peak (Fig. 3) is not sharp and appears to consist of overlapping two peaks separated by about 2–3 eV. It is well known that the s core-level photoemission peak of the $3d$ transition-metal ion with an incomplete $3d$ shell is split into two peaks due to the exchange interaction between the core hole and the $3d$ electrons.[11] Since the V $3s$ core levels of high-spin V^{3+} compounds show an exchange splitting of about 2.5 eV (Refs. 11 and 12) and the mean valence of V in V_5S_8 is 3.2+ (assuming the S ions to be 2−), the splitting of the V $3s$ peak would be attributed to the exchange splitting of the high-spin V^{3+} state. Thus, we fitted the V $3s$ spectrum using a 1:4 superposition of the spectra of high-spin V^{4+} and V^{3+} states (corresponding to the mean valence of 3.2+) as shown in Fig. 3(a). Here, the exchange splitting for each configuration is given by

$$\Delta E_{ex} \sim [(2S+1)/5]G^2(3s,3d)$$

and the intensity ratio of the two peaks is given by $S/(S+1)$, where S is the spin of the d^n configuration $(S=1$ for $V^{3+})$ and $G^2(3s,3d)$ is a Slater integral which

FIG. 2. S $2p$ core-level photoemission spectrum of V_5S_8. The measured spectrum (dots) is fitted to the theoretical line shape (solid curve) of a spin-orbit doublet ($\Delta E_{s.o.} = 1.15$ eV, $2\gamma = 0.54$ eV, $2G = 1.2$ eV, asymmetry parameter $\alpha = 0.18$) and a plasmon satellite.
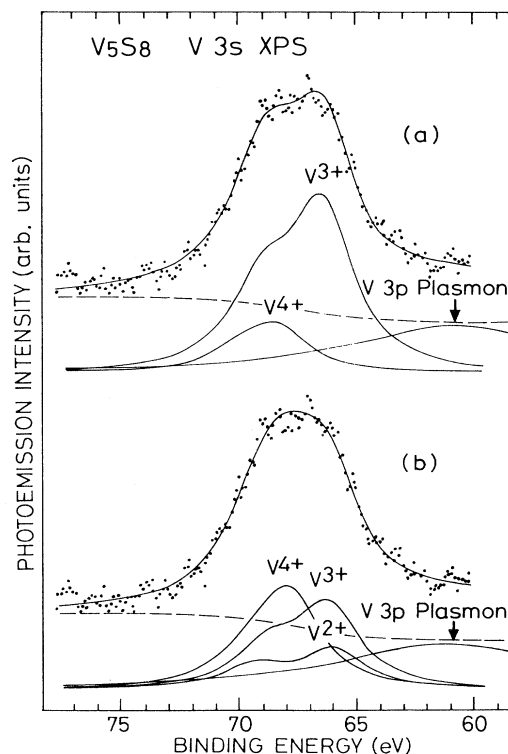
FIG. 3. V $3s$ core-level photoemission spectrum of V_5S_8 (dots). (a) Line-shape analysis assuming $V^{3+}:V^{4+}=4:1$ ($2\gamma = 2.9$ eV, $2G = 0.8$ eV, $\alpha = 0.0$); (b) line-shape analysis assuming $V^{2+}:V^{3+}:V^{4+}=1:2:2$ ($2\gamma = 2.8$ eV, $2G = 0.8$ eV, $\alpha = 0.0$). The broad feature centered at $E_B \sim 60$ eV is a plasmon satellite accompanying the V $3p$ core level.

we set to be 4.2 eV.[11] The presence of the overlapping V^{4+} component explains the observed intensity ratio of the two peaks larger than $S/(S+1)=\frac{1}{2}$. Another fit corresponding to the mean valence of $V^{3.2+}$ was also attempted using a 2:2:1 superposition of the V^{4+}, V^{3+}, and V^{2+} spectra as shown in Fig. 3(b). In the latter fit, the center of gravity of the V^{2+} component is slightly shifted toward higher binding energy than that of V^{3+}, contrary to what would be expected for core-level chemical shifts.

The V $2p$ core-level spectrum exhibits highly asymmetric $j=\frac{3}{2}$ and $\frac{1}{2}$ peaks as shown in Fig. 4. All attempts to fit the spectrum using a superposition of different valences as has been applied to mixed-valence V oxides[12,13] were not successful. Therefore, we assumed that the spectrum was dominated by an asymmetric broadening resulting from the screening of the core hole by conduction electrons,[14] but the asymmetry was found to be too strong to be fitted using a single peak having a standard asymmetric line shape.[15] According to Kotani and Toyozawa,[16] core-level photoemission from a narrow-band metal exhibits a two-peak structure as a result of two types of final states, namely, well-screened and poorly screened core-hole states depending on whether a local screening orbital (V $3d$, in this case) is occupied in the final state or not. Figure 4 shows such a tentative fit using two overlapping spin-orbit doublets. The poorly screened component (at higher binding energy) is broader than the well-screened one (at lower binding energy) because the former states decay into the latter states via an Auger-type process.

The absence of well-screened and poorly screened peaks in the V $3s$ spectrum would be due to the large spatial extent of the V $3s$ orbital compared to V $2p$. Because of the different sizes of the core orbitals, the attractive Coulomb energy between the V $3s$ hole and the V $3d$ elec-

tron would be much smaller than that between the V $2p$ hole and the V $3d$ electron and would not be strong enough to split a local screening orbital off the V $3d$ band. The weak V $3s$ core-hole potential is consistent with the vanishingly small asymmetry parameter (see caption for Fig. 3).

B. Valence band

Figure 5 shows the valence-band XPS and UPS spectra. Each spectrum shows the narrow occupied part of the V $3d$-t_{2g} conduction band with a resolution-limited Fermi cutoff and a broad S $3p$ band 1–8 eV below the Fermi energy (E_F). The observation of the sharp Fermi edge with a high density of states (DOS) indicates the presence of a sufficient amount of metallic electrons in this system. The separation between the V $3d$ and the S $3p$ bands is smaller than that between the V $3d$ and the O $2p$ bands in V oxides by 1.5–2.5 eV (see Fig. 6). This should lead to a stronger p-d hybridization in the sulfide than in the V oxides.

So far no band-structure calculation has been reported for V_5S_8. Therefore, we have simulated the DOS of paramagnetic V_5S_8 using that of VS (Refs. 17 and 18) or VS_2 (Ref. 19) by changing the relative weight of the DOS in the V $3d$- and S $3p$-band regions to represent the atomic ratio V/S$=5/8$ and by shifting E_F to accommodate the correct number of electrons. Considering the photoionization cross sections of the V $3d$ and S $3p$ atomic orbitals,[20] one can compare the He I spectrum with the total DOS. The intensity of the S $3p$ band is suppressed in the $h\nu=40.8$-eV spectrum due to a Cooper minimum in the S $3p$ atomic orbital cross section around this photon ener-
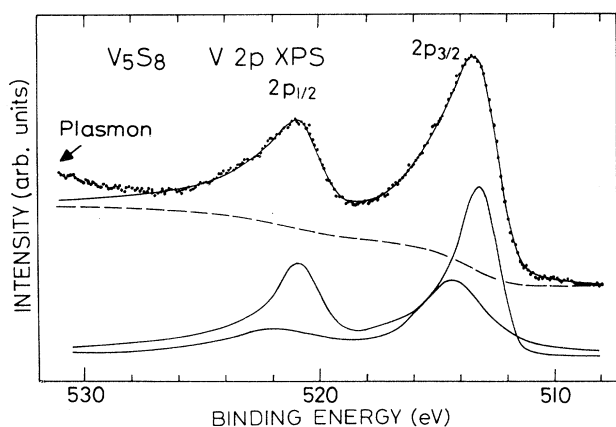
FIG. 4. V $2p$ core-level photoemission spectrum of V_5S_8. The measured spectrum (dots) is fitted using overlapping two spin-orbit doublets (solid curves). Line-shape parameters of the well-screened $2p_{3/2}$ peak are $2G=1.5$ eV, $2\gamma=0.24$ eV, $\alpha=0.4$, and those for the poorly screened $2p_{3/2}$ peak are $2G=1.5$ eV, $2\gamma=2.5$ eV, $\alpha=0$.
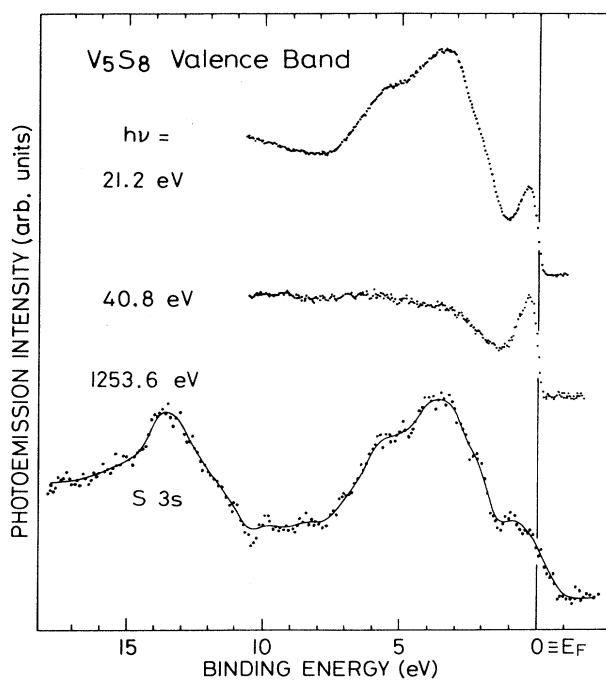
FIG. 5. Valence-band photoemission spectra of V_5S_8.

gy.[20] (This observation confirms the absence of O $2p$ emission due to contamination since the O $2p$ cross section monotonically increases with decreasing photon energy.) The He II spectrum can therefore be compared with the V $3d$ partial DOS. As shown in Fig. 6, we find good agreement between the experiment and band theory with respect to the width and the line shape of the V $3d$ conduction band as well as those of the S $3p$ band, suggesting that electron correlation is unimportant in V_5S_8. We note that good agreement between band theory and photoemission experiment has been reported for VS.[21] This is sharply contrasted with the spectrum of VO_2 in the metallic phase[22] shown in the same figure, where the measured V $3d$ conduction band is considerably broadened as compared to the calculated DOS (Ref. 23) due to significant electron correlation within the V $3d$ band.[24]

C. Auger-electron spectra

Core-valence-valence (CVV) Auger-electron spectra can be used to study the interactions between two holes
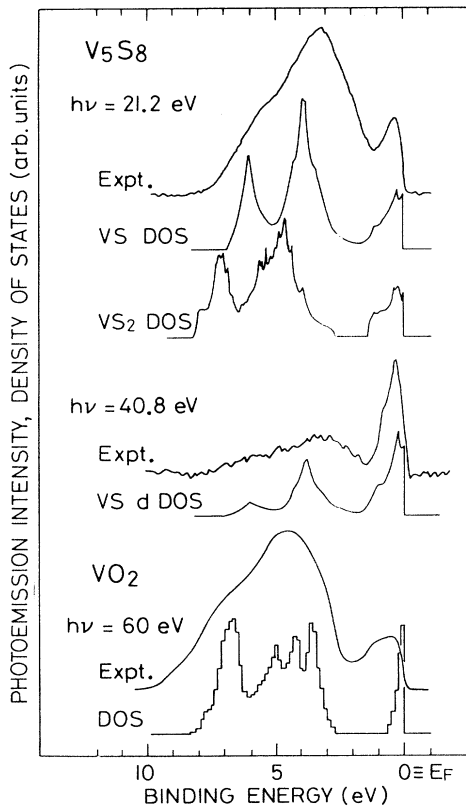
FIG. 6. Valence-band photoemission spectra of V_5S_8 compared with DOS given by band-structure calculations. The DOS of V_5S_8 have been synthesized from those of VS [Motizuki et al. (Ref. 18)] and that of VS_2 [Myron (Ref. 19)] as described in the text. Also shown is the valence-band UPS spectrum of VO_2 in the metallic phase [Shin et al. (Ref. 22)] and its calculated DOS [Gupta et al. (Ref. 23)]. Integral backgrounds have been subtracted from the experimental data.
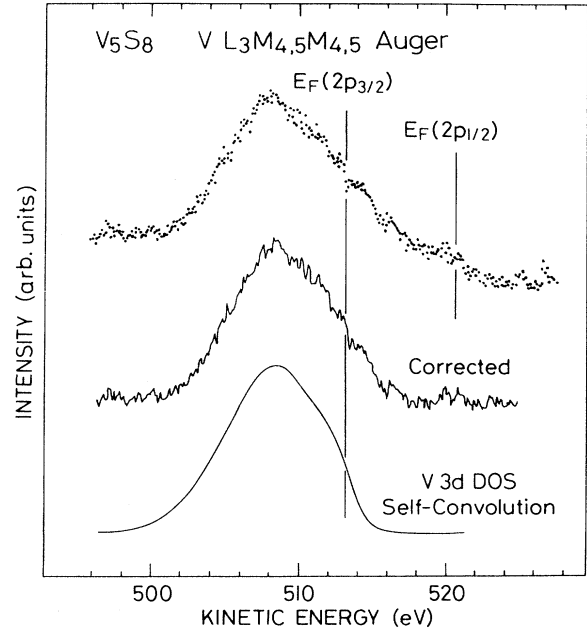
FIG. 7. V $L_3M_{4,5}M_{4,5}$ Auger-electron spectrum of V_5S_8 compared with the self-convolution of the He II UPS spectrum (broadened with a Gaussian function with $2G \sim 2.5$ eV in order to simulate the width of the initial core-hole state). The secondary-electron background and the L_2 component have been subtracted from the raw data (top) to yield the corrected curve (middle). $E_F(2p_{3/2})$ marks E_F for the $2p_{3/2}$ core-hole initial state, etc.

in the valence band or in the conduction band. In the absence of electron correlation, a CVV Auger spectrum involving a V core level is the self-convolution of the V $3d$ DOS, and electron correlation, if exists, distorts its line shape.[25] In Fig. 7, we compare the V $L_3M_{4,5}M_{4,5}$ ($2p_{3/2}$-$3d$-$3d$) Auger spectrum of V_5S_8 with the self-convolution of the He II UPS spectrum representing the V $3d$ partial DOS. One can see good agreement between the self-convolution and experiment without any sign of distortion, again implying that the electron correlation is not important.

IV. DISCUSSION

A. Electron correlation within the V $3d$ band

The valence-band photoemission and Auger-electron spectra suggest that d electrons in V_5S_8 are essentially itinerant and electron correlation is not important. The exchange splitting of the V $3s$ core-level spectrum, on the other hand, reveals atomic Hund's-rule coupling between $3d$ electrons in the ground state. These apparently contradicting results can be rationalized if one notices that, for high-spin configurations except for the half-filling (d^5), the effective d-d Coulomb energy U_{eff}, the lowest energy required for the charge fluctuation $d^n + d^n$

$\rightarrow d^{n+1}d^{n-1}$, is smaller than the average Coulomb energy U by the d-d exchange energy J, which is of the order of 1 eV, i.e., $U_{\text{eff}} = U - J$.[26] The photoemission results can be understood if $U_{\text{eff}} \ll W$ and $U \gtrsim W$: Under these conditions, a metallic d band is formed as a result of Hund's-rule coupling and therefore the coupling survives in the metallic state. The width of the V $3d$-t_{2g} band in V_5S_8 is estimated to be $W \sim 2$ eV from the band-structure calculations[17−19] (Sec. III B), and therefore we may infer that $U \sim 2$ eV and $U_{\text{eff}} = U - J \sim 1$ eV, which are similar to other estimates.[22,27,28]

Here, it should be noted that the on-site Coulomb energies in V_5S_8 are defined for electrons in antibonding states formed between the V $3d$-t_{2g} and the S $3p$ states and not for bare $3d$ electrons as in the case of (charge-transfer-type) late $3d$ transition-metal compounds.[29] This is one reason why the Coulomb energies in the V compounds ($U \sim 1$–2 eV) are much smaller than those in the late $3d$ transition-metal compounds ($U \sim 5$–8 eV).[29,30]

B. Implications for the magnetic properties

It has been controversial whether the magnetic properties of V_5S_8 are of the local-moment type or itinerant-electron type. According to the NMR studies,[7] only the V^I site has a local moment and the V^{II} and V^{II} sites (constituting 80% of the total V atoms) are believed to be nonmagnetic. The exchange splitting of the V $3s$ core-level peak indicates that the nonmagnetic behavior of the V^{II} and V^{III} sites is not due to an atomic low-spin configuration but due to an intersite coupling between the V local moments. (The dynamical fluctuation of the V^{II}- and V^{III}-site moments should be slow compared to the time scale of photoemission for the exchange splitting to be observed.) Magnetotorque measurements below T_N have indicated that the c axis is the easy magnetization axis but that the magnetic anisotropy energy is very small, ~ 0.24 cm^{-1}.[3]

As for the possible valences of the V^I ion, we shall consider V^{2+}, V^{3+}, and V^{4+}. In Table I, we list their effective moments to compare with that of the paramagnetic state. Such ionic models may not be fully justified because of the strong V $3d$–S $3p$ hybridization and possible itinerancy of d electrons, but in the following we shall take these models as a well-defined starting point and

consider the deviations from it when they become necessary.

In order to discuss the magnetic anisotropy in the antiferromagnetic state, we consider the splitting of the V $3d$-t_{2g} level under the trigonal crystal filed as shown in Fig. 8. The VS_6 unit is elongated along the c axis,[8] which will lower the $3z^2$-r^2 level relative to the doubly degenerate xy, x^2-y^2 level through the anisotropic V $3d$–S $3p$ hybridization. Furthermore, positive V^{II} ions are located above and below the V^I ion, which will also lower the $3z^2$-r^2 level relative to the others.

If the V^I ion is in the high-spin V^{2+} state, it is magnetically isotropic in agreement with experiment [Figs. 8(c) and 8(f)]. For the high-spin V^{2+} state, $U_{\text{eff}} = U - J + 10Dq$ ($10Dq$: cubic crystal-filled splitting), which is much larger than those for V^{3+} and V^{4+} ($U_{\text{eff}} = U - J$) and would explain why V $3d$ electrons are localized only at the V^I site. The effective moment of V^{2+}, however, is too large compared to the experimental value (Table I).

The effective moment of the V^{3+} ion is close to the experimental value. The small discrepancy could be due to an incomplete quenching of the angular momentum (see Table I). In this case, d electrons are localized at the V^I site probably because of the relatively isolated structural environment and hence the effectively reduced d-band width at this site. However, the magnetic anisotropy energy of the V^{3+} ion in the trigonal crystal field is too large to explain the observed small anisotropy unless the trigonal crystal-field splitting Δ is unreasonably large (of the order of ~ 5 eV).[3] [The V^{3+} ion remains anisotropic even if the sign of Δ were negative as shown in Fig. 8(b).]

TABLE I. Effective moments and the ordered spin moments of V (in μ_B).

| | Effective Bohr magneton | | |
	Spin only (ion in crystal)	Spin+orbital (free atom)	Ordered magnetic moment
V^{2+}	3.87	0.77	3.0
V^{3+}	2.83	1.63	2.0
V^{4+}	1.73	1.55	1.0
V_5S_8 (expt.)	~ 2.3[a]		0.22[b] 0.7–1.5[c]

[a]Reference 3.
[b]NMR (Ref. 4).
[c]Neutron diffraction (Ref. 6).
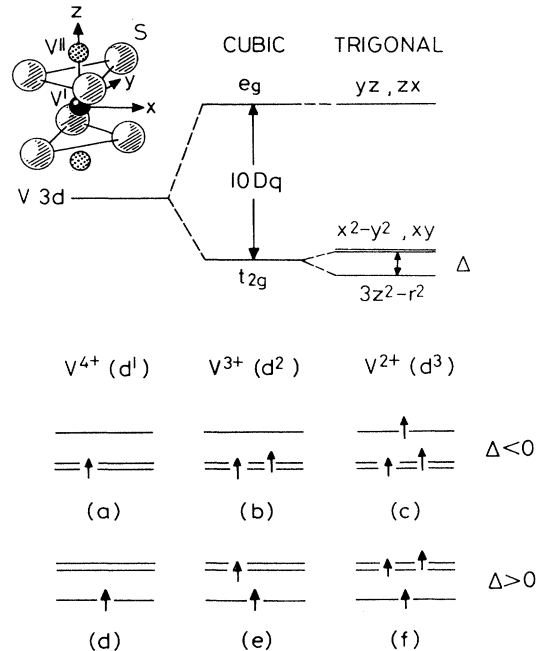
FIG. 8. Schematic energy-level diagrams for the V^I ion in V_5S_8. The trigonal crystal-field splitting Δ is probably positive.

The ground state of the V^{4+} ion is magnetically isotropic for the present trigonal crystal field [Fig. 8(d)].[3] However, the effective moment of the V^{4+} ion is too small to account for the paramagnetic susceptibility (Table I).

From the crystal structural point of view, we note that the three V sites have nearly the same average V-S distances (V^I: 2.399 Å, V^{II}: 2.384 Å, V^{III}: 2.390 Å).[8] If the V^I ion is V^{3+}, the average valence of the V^{II} and V^{III} ions becomes 3.25+. This rather uniform valence distribution is consistent with the structural data. If V^I is 4+, the average valence of V^{II} and V^{III} is 3+; if V^I is 2+, it is 3.5+. In the latter two cases, the V-S distance should be quite different for the different V sites in the ionic model, since the ionic radius significantly differs for the different valences (V^{2+}: 0.79 Å, V^{3+}: 0.64 Å, and V^{4+}: 0.59 Å).[31]

Thus, the crystal structure and the paramagnetic behavior favor the V^I site being V^{3+}, whereas none of the ionic models can account for the antiferromagnetic states in a way consistent with the paramagnetic state. This suggests that the local-moment picture is insufficient to describe the antiferromagnetic state in V_5S_8. In the antiferromagnetic state, partial delocalization of the V^I-state local moment possibly occurs, which might be related to the small magnetic anisotropy. Such a delocalization may be the origin of the small V^I-site ordered moment as determined by NMR ($0.22\mu_B$) (Ref. 4) compared to that estimated by neutron diffraction [$(0.7-1.5)\mu_B$]:[6] The former value has been obtained from the hyperfine coupling constant above T_N and the hyperfine filed at the V^I site below T_N under the assumption that the coupling constant does not change across T_N. Therefore, the small ordered moment deduced from NMR is most probably due to a change in the hyperfine coupling constant across T_N, and such a change would result from a change in the character of d electrons in going from the paramagnetic state to the antiferromagnetic state. This "weakly itinerant" antiferromagnetism is considered to be intermediate between the weak antiferromagnetism as described by the self-consistent-renormalization spin-fluctuation theory[32] in the weak-correlation limit and the local-moment antiferromagnetism in the strong-correlation limit.

V. CONCLUSION

We have studied the electronic structure of an antiferromagnetic metal V_5S_8 above the Néel temperature by photoemission and Auger-electron spectroscopy. The exchange splitting of the V 3s core-level spectrum is interpreted as due to a mixture of high-spin d^1, d^2, and possibly d^3 configurations in the ground state, whereas the valence-band photoemission spectra show a sharp Fermi edge and are in good agreement with the DOS given by the band-structure calculations. In order to explain these observations in a consistent way, we have proposed that the effective on-site Coulomb energy for the Hund's-rule ground states of the V^{4+} (d^1) and V^{3+} (d^2) configurations $U_{eff} = U - J$ is smaller than the one-electron t_{2g} bandwidth even if the average Coulomb energy U may be comparable to or exceed the bandwidth.

The d electrons at the V^I site appear to behave as a localized high-spin V^{3+} (d^2) configuration at least in the paramagnetic state, whereas partial delocalization or weak itinerancy of the same d electrons would have to be taken into account in order to understand the antiferromagnetic state.

ACKNOWLEDGMENTS

[1]Y. Kitaoka and H. Yasuoka, J. Phys. Soc. Jpn. **48**, 1949 (1980).

[2]A. B. De Vires and C. Haas, J. Phys. Chem. Solids **34**, 651 (1972).

[3]H. Nozaki, M. Umehara, Y. Ishizawa, M. Saeki, T. Mizoguchi, and M. Nakahira, J. Phys. Chem. Solids **39**, 851 (1978).

[4]Y. Kotaoka, H. Yasuoka, K. Oka, K. Kosuge, and S. Kachi, J. Phys. Soc. Jpn. **46**, 1381 (1979).

[5]H. Nozaki, Y. Ishizawa, M. Saeki, and M. Nakahira, Phys. Lett. **54A**, 29 (1975).

[6]S. Funahashi, H. Nozaki, and I. Kawada, J. Phys. Chem. Solids **42**, 1009 (1981).

[7]B. G. Silbernagel, R. B. Levy, and F. R. Gamble, Phys. Rev. B **11**, 4563 (1975).

[8]I. Kawada, M. Nakano-Onoda, and M. Saeki, J. Solid State Chem. **15**, 246 (1975).

[9]M. Saeki, M. Nakano, and M. Nakahira, J. Cryst. Growth **24/25**, 154 (1974).

[10]M. O. Krause and J. H. Oliver, J. Phys. Chem. Ref. Data **8**, 329 (1979).

[11]D. A. Shirley, in *Photoemission in Solids I,* edited by M. Cardona and L. Ley (Springer-Verlag, Berlin, 1978), p. 167.

[12]A. Fujimori, K. Kawakami, and N. Tsuda, Phys. Rev. B **38**, 7889 (1988).

[13]M. Nakamura, A. Misu, H. Namatame, A. Fujimori, S. Naka, and H. Nagasawa (unpublished).

[14]G. K. Wertheim and P. H. Citrin, *Photoemission in Solids I,* Ref. 11, p.197.

[15]G. D. Mahan, Phys. Rev. B **11**, 4814 (1975).

[16]A. Kotani and Y. Toyozawa, J. Phys. Soc. Jpn. **37**, 912 (1974).

[17]J. Nakahara, H. Franzen, and D. K. Misemer, J. Chem. Phys. **76**, 4080 (1982).

[18]K. Motizuki, K. Kato, and A. Yanase, J. Phys. **19**, 495 (1986).

[19]H. W. Myron, Physica B **99**, 243 (1980).

[20]J. J. Yeh and I. Lindau, At. Data Nucl. Data Tables **32**, 1 (1985). The calculated S 3p cross section has to be multiplied by a factor of ~ 2 when compared with experiment [A. Fujimori, M. Sekita, and M. Saeki, Phys. Rev. B **33**, 6652 (1986)]. As a result, the V 3d and S 3p cross sections per elec-

tron are nearly the same for $h\nu = 21.2$ eV, and the S $3p$ cross section per electron is only $\sim 10\%$ of that of V $3d$ for $h\nu = 40.8$ eV.

[21]H. F. Franzen and G. A. Sawatzky, J. Solid State Chem. **15**, 229 (1975).

[22]S. Shin, S. Suga, M. Taniguchi, M. Fujisawa, H. Kanzaki, A. Fujimori, H. Daimon, Y. Ueda, K. Kosuge, and S. Kachi, Phys. Rev. B **41**, 4993 (1990).

[23]M. Gupta, A. J. Freeman, and D. E. Ellis, Phys. Rev. B **16**, 3338 (1977).

[24]S. R. White, D. J. Scalapino, R. L. Sugar, and N. E. Bickers, Phys. Rev. Lett. **63**, 1523 (1989); B. Menge and E. Müller-Hartmann, Z. Phys. B **82**, 237 (1991).

[25]G. A. Sawatzky and A. Lenselink, Phys. Rev. B **21**, 1790

(1980).

[26]The energies of the Hund's-rule ground states of V ions are $E(d^1) = \epsilon_d$, $E(d^2) = 2\epsilon_d + U - J$, $E(d^3) = 3\epsilon_d + 3U - 3J$, $E(d^4) = 4\epsilon_d + 6U - 6J + 10Dq$, and U_{eff} for d^n is given by $E(d^{n+1}) + E(d^{n-1}) - 2E(d^n)$.

[27]G. A. Sawatzky and D. Post, Phys. Rev. B **20**, 1546 (1979).

[28]C. Sommers and S. Doniach, Solid State Commun. **28**, 133 (1978).

[29]J. Zaanen, G. A. Sawatazky, and J. W. Allen, Phys. Rev. Lett. **55**, 418 (1985); S. Hufner, Z. Phys. B **58**, 1 (1984).

[30]A. Fujimori and F. Minami, Phys. Rev. B **30**, 957 (1984).

[31]R. D. Shannon and C. T. Prewitt, Acta Crystallogr. B **52**, 925 (1969).

[32]H. Hasegawa and T. Moriya, Phys. Soc. Jpn. **36**, 1542 (1974).